QUANTUM MEASUREMENTS OF TRAPPED IONS*

W. M. Itano, J. C. Bergquist, J. J. Bollinger, J. M. Gilligan, D. J. Heinzen,†
F. L. Moore,† M. G. Raizen† and D. J. Wineland

Time and Frequency Division, National Institute of Standards and Technology, Boulder,
CO 80303, U.S.A.

When a quantum state is subjected to a measurement and the state is not
an eigenstate of the dynamical variable being measured, the outcome is unpre-
dictable. Only the probabilities of the various possible outcomes are predicted by
theory. This phenomenon is sometimes discussed in terms of "wavefunction col-
lapse." Trapped ions can be used for real, as opposed to *gedanken* demonstrations
of this basic process. In the experiments described here, a single ion, or a few
identical ions, were prepared in well defined superpositions of two internal energy
eigenstates. The populations of the energy levels were then measured. When
the state amplitudes were equal, the population fluctuations were greater than
when one of the amplitudes was nearly zero, in agreement with the predictions of
quantum mechanics. In other experiments, such as those with atomic beams, the
number of atoms under observation fluctuates, and this obscures the fluctuations
from other sources. However, if the number of atoms is small and constant, the
fundamental quantum mechanical fluctuations can be observed.

INTRODUCTION

This article is a preliminary report on some quantum measurement experiments on trapped ions
that have been performed at the National Institute of Standards and Technology. An article
containing more complete discussions of the theory and experiment is in preparation (Itano *et
al.*, 1992). Trapped ions (ions suspended in space by electric and magnetic fields) are quantum
systems that are particularly well isolated from the environment. Thus, they are well suited for
various tests of fundamental physical principles. [For a recent review, see (Blatt *et al.*, 1992).]

Quantum mechanics does not, in general, predict the result of an experiment. Rather, it provides
a prescription for predicting the *probability* of observing a given result. Perhaps the simplest
example of the indeterminism of quantum mechanics is the behavior of a two-level system prepared
in a superposition $|\psi\rangle = c_A|A\rangle + c_B|B\rangle$ of the two states $|A\rangle$ and $|B\rangle$, which is subjected to a
measurement. The measurement yields one indication or "pointer reading" for a system in $|A\rangle$

---

*Work of the U. S. Government. Not subject to U. S. copyright.
†Present address: Department of Physics, University of Texas, Austin, TX 78712.

and another for a system in $|B\rangle$. Except when either c_A or c_B is zero, the outcome of the measurement cannot be predicted with certainty. Provided that the state vector is properly normalized ($|c_A|^2 + |c_B|^2 = 1$), $|c_A|^2 \equiv p_A$ and $|c_B|^2 \equiv p_B$ are the probabilities of finding the system in $|A\rangle$ or $|B\rangle$, respectively. The indeterminacy is present no matter how accurately the state has been prepared. It is an inherent feature of quantum mechanics. We will call this source of measurement fluctuations "projection noise," since it arises from the random projection of the state vector into one of the states compatible with the measurement process.

In some experiments, we have a sample of N identical systems which are effectively independent. If we carry out the same kind of state preparation and measurement as that just described for a single system, then we should get the same result as repeating the experiment N times. That is, the total number of atoms in a given state should have the same mean and fluctuations as would be obtained from N independent measurements on one system.

If the N atoms are uncorrelated, the fluctuations of the measured populations can be calculated by combining the probabilities according to the binomial distribution (Bevington, 1969). [The same result is obtained by explicitly projecting the N-atom state, which is an atomic coherent state (Arecchi et al., 1972) onto the states of definite $|A\rangle$ and $|B\rangle$ populations (the Dicke states) (Itano et al., 1992).] Let N_A and N_B be the numbers of atoms found to be in $|A\rangle$ and $|B\rangle$, respectively ($N_A + N_B = N$).

Then, according to the binomial distribution, the probability of measuring a given value of N_B is

$$P(N_B, N, p_B) = \frac{N!}{N_B!(N - N_B)!}(p_B)^{N_B}(1 - p_B)^{(N-N_B)}, \tag{1}$$

where $p_B \equiv |c_B|^2$ is the probability for a single atom to be in $|B\rangle$ and $(1 - p_B) = p_A \equiv |c_A|^2$ is the probability to be in $|A\rangle$. The variance of the binomial distribution is (Bevington, 1969)

$$\sigma^2 = Np_B(1 - p_B). \tag{2}$$

The variance is zero when $p_B = 0$ or $p_B = 1$ and has its maximum value of $N/4$ when $p_B = 1/2$. Equation (1) is valid for the special case where there is only one atom ($N = 1$). In this case, N_B can have only two values, 0 or 1.

Equation (1) was derived for an uncorrelated N-atom system in which all of the atoms have the same state vector. For more general states, in which the state vectors of different atoms are correlated with each other, it may be possible for the variance to be either larger or smaller than this value (Kitagawa and Ueda, 1991; Yurke, 1986; Yurke et al., 1986; Wineland et al., 1992). Such states are analogous to the better-known squeezed states of the electromagnetic field.

SINGLE-ATOM EXPERIMENT

Quantum state preparation and detection experiments were carried out with ^{199}Hg$^+$ ions confined in a linear rf trap. Detailed observations were made of single ions, although some experiments were also carried out with several independent but simultaneously trapped ions.
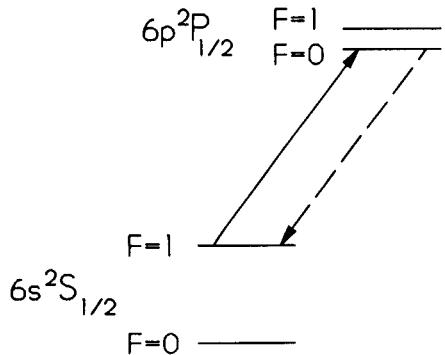
Figure 1: Energy levels of ^{199}Hg$^+$. The transition between the $^2S_{1/2}$ and $^2P_{1/2}$ states is at 194 nm. The hyperfine splittings in the $^2S_{1/2}$ and $^2P_{1/2}$ states are 40.5 GHz and 6.9 GHz, respectively. The $^2S_{1/2}$ ($F = 1$) state is detected by exciting the $^2S_{1/2}$ ($F = 1$) → $^2P_{1/2}$ ($F = 0$) transition.

^{199}Hg$^+$ Energy Levels

Figure 1 shows the energy levels of ^{199}Hg$^+$ which were important for the experiments. The ground electronic state has the configuration $5d^{10}6s\,^2S_{1/2}$. The first electric dipole transition, at 194 nm, is to the $5d^{10}6p\,^2P_{1/2}$ state. The ^{199}Hg nucleus has spin 1/2, so both the $^2S_{1/2}$ and the $^2P_{1/2}$ states are split by hyperfine interactions into states with total angular momentum $F = 0$ and $F = 1$. For both the $^2S_{1/2}$ and $^2P_{1/2}$ states, the ($F = 1$) hyperfine state is higher in energy than the ($F = 0$) hyperfine state. The $^2S_{1/2}$ hyperfine splitting has been measured by microwave resonance methods to be 40 507 347 996 9±0.3 Hz (Cutler *et al.*, 1981). The $^2P_{1/2}$ hyperfine splitting has been measured by Fabry-Pérot interferometry to be 6 955±90 MHz (Guern *et al.*, 1977). The natural linewidth of the $^2P_{1/2}$ state is about 70 MHz (Eriksen and Poulsen, 1980; Itano *et al.*, 1987).

Apparatus

The ^{199}Hg$^+$ ions were confined in a linear rf trap which has been described previously (Raizen *et al.*, 1992). It consisted of four parallel cylindrical electrodes of radius 0.794 mm arranged symmetrically around a central axis. The distance from the central axis to the surface of the electrodes was 0.769 mm. The rf potentials on any two adjacent electrodes were 180° out of phase. The amplitude of the rf potential was about 500 V and its frequency was 12.7 MHz. The electric fields produced by these electrodes created a force which pushed the ions to the central axis. The electrodes were divided into sections, to which static electric potentials of 1 V or less were applied to keep the ions from escaping along the axis.

Ions were produced by electron impact ionization of neutral atoms inside the trap volume. A sample of ^{199}Hg of isotopic purity 91% was used. Typically, the pressure was about 10^{-7} Pa (1 Pa ≈ 7.5 mTorr), except when the ions were being created, when it was raised to a higher level. The ions were confined to a region of a few hundred micrometers extent around the center of the

trap. After being laser-cooled, a single ion was localized in position to about 1 μm or less.

Narrowband, cw radiation at 194 nm was required for laser-cooling and optical detection of the ^{199}Hg$^+$ ions. This was generated by a combination of second-harmonic generation and sum-frequency mixing, starting with cw lasers (Hemmati *et al.*, 1983). About 5 μW of 194 nm radiation was available. In order to laser-cool and continuously observe the ions, 194 nm radiation near both the $^2S_{1/2}$ ($F = 1$) $\rightarrow$ $^2P_{1/2}$ ($F = 0$) and the $^2S_{1/2}$ ($F = 0$) $\rightarrow$ $^2P_{1/2}$ ($F = 1$) transition wavelengths was required (Raizen *et al.*, 1992). We call these two sources laser 1 and laser 2. If only one laser was present, the ions were optically pumped to a hyperfine state which could not absorb the 194 nm radiation. Also, in order to prevent trapping of the ions in Zeeman sublevels of the $^2S_{1/2}$ ($F = 1$) state, it was necessary to apply a magnetic field of approximately 5×10^{-4} T at an angle of approximately 45° with respect to the electric field polarization of the $^2S_{1/2}$ ($F = 1$) $\rightarrow$ $^2P_{1/2}$ ($F = 0$) 194 nm radiation.

Some of the 194 nm radiation emitted by the ions perpendicular to the trap axis was focused by a multi-element lens onto a two-dimensional imaging photon-counting tube. The probability of a photon emitted by an ion being detected was about 10^{-4}. Individual ions could be resolved with this apparatus. Some images showing several clearly resolved ions have been published previously (Raizen *et al.*, 1992). From the size of the image of a single ion, it could be inferred that the temperatures were not much greater than the theoretical values of a few millikelvins (Itano and Wineland, 1982; Wineland and Itano, 1987). The electronics could be adjusted so that the photons from any rectangular region of the image, for example a region including only one ion, could be counted separately.

State Preparation and Detection

Optical pumping can be used to prepare the ions in either the ($F = 1$) or the ($F = 0$) hyperfine level of the $^2S_{1/2}$ ground state. In order to prepare them in the ($F = 1$) state, both laser 1 and laser 2 are left on. If an ion in the ground ($F = 1$) state is excited to the $^2P_{1/2}$ ($F = 0$) state, it is forbidden by electric dipole selection rules from decaying to the ground ($F = 0$) state and must return to the ($F = 1$) state. There is a weak transition rate from the ground ($F = 1$) state to the ground ($F = 0$) state, via the $^2P_{1/2}$ ($F = 1$) virtual state. This rate is approximately 3×10^{-5} times the rate of leaving the ground ($F = 1$) state and returning to the same state, via the $^2P_{1/2}$ ($F = 0$) state, since laser 1 is far from resonance with the $^2S_{1/2}$ ($F = 1$) $\rightarrow$ $^2P_{1/2}$ ($F = 1$) transition. If an ion does make a transition to the ground ($F = 0$) state, laser 2 quickly drives it back to the $^2P_{1/2}$ ($F = 1$) state, which decays, with probability 2/3, to the ground ($F = 1$) state. If laser 1 and laser 2 are both turned off at the same time, the ion will be in the ground ($F = 1$) state with high probability, after a few multiples of the $^2P_{1/2}$ state lifetime (2.3 ns). This method does not select a particular M_F Zeeman sublevel of the ground ($F = 1$) state.

An ion can be prepared in the $^2S_{1/2}$ ($F = 0$) hyperfine level by turning off laser 2 while leaving laser 1 on. For a typical intensity of laser 1, the ion is pumped to the ground ($F = 0$) state in about 10 ms. In contrast to the previous method, the ion is prepared in a single M_F state. Laser 1 can also pump an ion from the ground ($F = 0$) state to the ground ($F = 1$) state. However, the rate for ($F = 0$) $\rightarrow$ ($F = 1$) is less than for ($F = 1$) $\rightarrow$ ($F = 0$), mainly because laser 1 is farther from resonance for this process. In the steady state, the probability of being in the ($F = 0$) state is about 94%. After the ion was prepared in the ground ($F = 0$) state, any desired superposition with the ground ($F = 1, M_F = 0$) state could be created by applying rf fields, at approximately 40.5 GHz, having well-controlled frequency, amplitude, and duration.
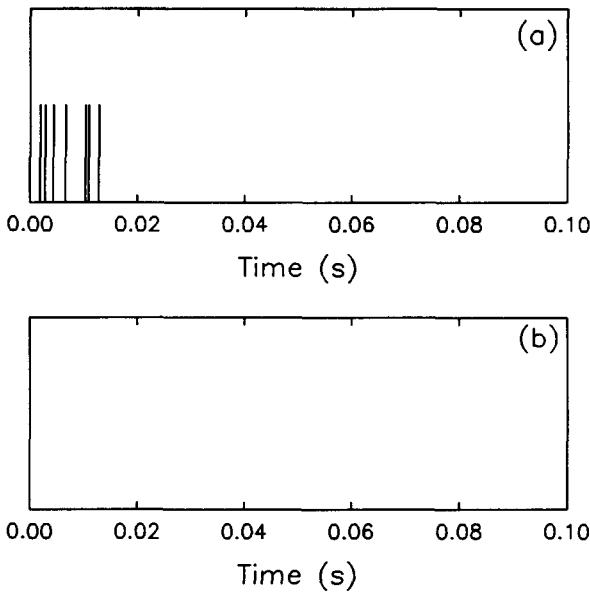
Figure 2: Typical record of the detected photons from a single $^{199}\text{Hg}^+$ ion prepared in the ground (a) $(F = 1)$ state and (b) $(F = 0)$ state. The horizontal axis represents the time after laser 1, the detection laser, is turned on. Each vertical line represents the detection of a single photon. In (a), eight photons were detected (two photons were too close in time to resolve on the graph). In (b), no photons were detected.

State detection was carried out by counting the 194 nm photons emitted by the ions for a period, typically 15 ms, with laser 1 turned on and laser 2 turned off. The mean number of photons detected was proportional to the number of ions in the $(F = 1)$ state. This is an example of electron-shelving detection (Dehmelt, 1982). For many ions, this signal is subject to fluctuations due to statistical fluctuations in the number of photons detected as well as laser intensity fluctuations.

Quantitative studies were made with only a single ion. In this case, the ion was determined to be in the $(F = 1)$ state if some photons were detected and in the $(F = 0)$ state if no photons were detected. There was some possibility of error with this detection method. A dark count from the phototube or a detected photon scattered from some surface could lead to a false $(F = 1)$ signal. Also, since the mean number of photons detected from an $(F = 1)$ ion was small (typically about 5), it was possible that none of them would be observed, thus leading to a false $(F = 0)$ signal. If the detection efficiency could be improved, both of these problems could be reduced by using a higher threshold number of photons to distinguish $(F = 1)$ and $(F = 0)$.

Results

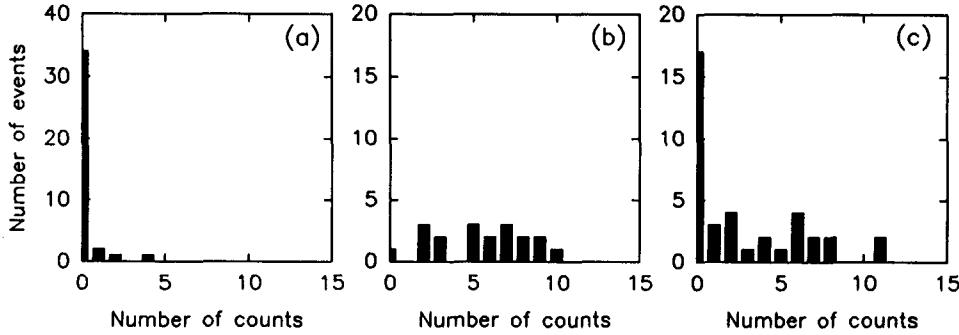The ability to prepare an ion in either the $(F = 0)$ or $(F = 1)$ ground hyperfine state is shown

Figure 3: Photon count distributions for a single $^{199}\text{Hg}^+$ ion prepared in (a) the $(F = 0, M_F = 0)$ state (b) the $(F = 1, M_F = 0)$ state (c) an equal superposition of these two states. The bars represent the number of cases in which a given number of fluorescence photons were detected when the detection laser was applied.

in Fig. 2. Each vertical line denotes the detection of a single photon at a particular time. The detection electronics were adjusted so that only photons from a single ion were detected. Before recording the data shown in Fig. 2(a), the ion was prepared in the ground $(F = 1)$ state by leaving both laser 1 and laser 2 on for about 0.1 s and then turning them off together. After a short delay, laser 1 was turned on, and for 0.1 s, the photons were counted. Their detection times were recorded with a resolution of 100 μs. In the example shown in Fig. 2(a), eight photons were recorded, but two of them were too close in time to be resolved on the graph. Before recording the data shown in Fig. 2(b), the ion was prepared in the ground $(F = 0)$ state by leaving laser 1 on and laser 2 off for 0.05 s. Laser 1 was then turned off. After a short delay, laser 1 was turned back on again, and the computer was set to record photons, as for the Fig. 2(a). No photons were recorded, indicating that the ion was in the $(F = 0)$ state.

Figure 3 shows the distributions of the numbers of photons detected after the single ion was prepared in different superposition states. Figure 3(a) shows the distribution for a nearly pure $(F = 0)$ state. In most cases, no photons were observed. However, in a few cases (4 out of 38) one or more photons were observed, presumably due to a combination of background scattered light and imperfect state preparation. Figure 3(b) shows the distribution when the ion was prepared in a nearly pure $(F = 1, M_F = 0)$ state. There is a broad distribution of numbers of photons detected, with a mean of about 5.5. There was one measurement (out of 19) in which no photons were measured. This may have been due to imperfect state preparation or to the possibility that no photons were detected, even though some were emitted. Figure 3(c) shows the distribution for the case when the state was a superposition with approximately equal amplitudes for $(F = 0)$ and $(F = 1, M_F = 0)$. The distribution is a superposition of those for $(F = 0)$ and $(F = 1, M_F = 0)$, with about equal weights. Out of 38 measurements, there were 17 in which no photons were detected. This bimodal distribution is the signature of the projection noise for the single-atom case. That is, for a superposition state with equal amplitudes of the two components, the measurement finds the ion randomly in one state or the other with equal probabilities.

Discussion

The two-state, single-atom case is special (or trivial), since the mean populations and the fluctuations about the mean are so closely connected. If $p_B = 1/2$, it means that a measurement must find the atom in $|B\rangle$ half the time and in $|A\rangle$ half the time. The population fluctuations are then maximal. If $p_B = 1$, a measurement will find the atom in $|B\rangle$ every time. The population fluctuations are then minimal. The case of arbitrary p_B is given by a simple calculation. Define the operator P_B as $|B\rangle\langle B|$. The mean value of this operator, $\langle P_B \rangle$, is p_B. The variance is

$$
\begin{aligned}
\sigma^2 &= \langle P_B^2 \rangle - \langle P_B \rangle^2 = \langle P_B \rangle - \langle P_B \rangle^2 \\
&= p_B - p_B^2 = p_B(1 - p_B),
\end{aligned}
\tag{3}
$$

which is the same as Eq. (2) for $N = 1$. The fact the $P_B^2 = P_B$ was used in Eq. (3). Thus, the projection noise in the single-atom case follows automatically from the assumption that there are only two possible states. [For the N-atom case, an additional assumption of lack of correlation among the atoms is required to obtain Eq. (1) and Eq. (2).] As a counterexample, a consider the correlated state of two atoms $(|A\rangle_1|B\rangle_2 + |B\rangle_1|A\rangle_2)/\sqrt{2}$, where the subscripts 1 and 2 label the atoms. A measurement will find one atom in $|A\rangle$ and the other one in $|B\rangle$, although it is uncertain *which* atom will be in $|A\rangle$ and which will be in $|B\rangle$. The population fluctuations will then be zero.

N-ATOM EXPERIMENT

N-atom quantum state preparation and detection methods were carried out with ^{9}Be$^+$ ions in a Penning trap. The Penning trap was used, rather than the rf trap, because the number of ions that could be stably trapped could be varied from a few to several thousand. During the time of the experiment, the number of trapped ions remained nearly constant. However, loading and detecting single ions was difficult with this apparatus.

^{9}Be$^+$ Energy Levels

Figure 4 shows the energy levels of ^{9}Be$^+$ which were important for the experiments. The ground electronic state has the configuration $2s\,^2S_{1/2}$. The ^{9}Be nucleus has spin 3/2, so that there are a total of 8 ground-state hyperfine-Zeeman states. In a high magnetic field, as is present in the Penning trap, the energy eigenstates are approximate eigenstates of I_z and J_z, the z-components of the nuclear and electronic angular momenta. The static magnetic field direction defines the z-axis. These eigenstates will be referred to by their main components in the $|M_I, M_J\rangle$ basis. For brevity, they will also be referred to by numbers 1–8, as shown in Fig. 4, which correspond, in order of decreasing energy, to $|-3/2, +1/2\rangle$, $|-1/2, +1/2\rangle$, $|+1/2, +1/2\rangle$, $|+3/2, +1/2\rangle$, $|+3/2, -1/2\rangle$, $|+1/2, -1/2\rangle$, $|-1/2, -1/2\rangle$, and $|-3/2, -1/2\rangle$. The 313 nm transition to the $2p\,^2P_{3/2}$ electronic state was used for state selection and detection.

Apparatus

The experimental apparatus and techniques have been described previously (Bollinger *et al.*, 1989; Gilbert *et al.*, 1988; Bollinger *et al.*, 1991; Itano *et al.*, 1990). The Penning trap was made of cylindrical electrodes, to which static electric potentials were applied. It was inserted into the bore of a superconducting solenoid magnet, which generated a uniform magnetic field B_0 of
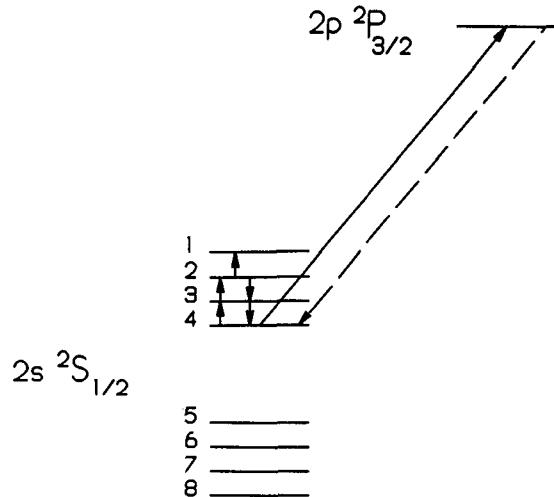
Figure 4: Level diagram for ^{9}Be$^+$. The ground state Zeeman-hyperfine states are labeled by numbers 1–8. Their quantum numbers are given in the text. Laser radiation at 313 nm optically pumps most of the ions into state 4. These ions are then transferred to state 3 and then to state 2 by rf π-pulses. Other rf pulses then create a superposition of states 1 and 2. Ions which remain in state 2 are transferred back to state 4. The laser radiation is applied again, and the number of ions in state 4 is determined from the fluorescence intensity.

approximately 0.82 T. The combination of the electrostatic potentials and uniform magnetic field trapped the ions in three dimensions. The pressure in the trap was approximately 10^{-8} Pa. The ions were created by electron impact ionization of neutral atoms.

Fluorescence from the ions was focused by a multi-element lens onto the photocathode of an imaging photon-counting tube. The overall detection efficiency was approximately 2×10^{-4}.

Ion Number Measurement

In the ^{199}Hg$^+$ experiments, the number of ions could be determined directly from the image. This could not be done for the ^{9}Be$^+$ ions in the Penning trap, since they rotate rapidly around the z axis. Therefore the number was determined indirectly. Calculations based on a charged fluid model relate the density of the ion plasma to its shape, for given external fields (Wineland *et al.*, 1985; Larson *et al.*, 1986). The shape and size of the ion plasmas were determined by moving the laser beam and observing the imaged fluorescence. The product of the density and volume yielded the number of ions with an uncertainty estimated to be about 30%.

State Preparation and Detection

In the ^{9}Be$^+$ experiments, coherent superpositions of two internal states (states 1 and 2) were

created and then subjected to measurements. These states were chosen because, for a value of B_0 near 0.8194 T, the first derivative of the transition frequency with respect to B_0 goes through zero. The resulting insensitivity to magnetic field fluctuations makes it easier to generate coherent superposition states reproducibly.

The state preparation began by subjecting the ions to 313 nm radiation, polarized perpendicular to the magnetic field, for approximately 15 s. The frequency of the 313 nm radiation was slightly below the $2s\,^2S_{1/2}$ $(M_I = +3/2, M_J = +1/2) \rightarrow 2p\,^2P_{3/2}$ $(M_J = +3/2, M_I = +3/2)$ transition frequency. This is a cycling transition, since electric dipole selection rules require that the ion return to the ground state sublevel that it started from. Spontaneous Raman transitions, induced by the 313 nm radiation, established a steady state in which approximately 16/17 of the ions were in state 4 and the remaining 1/17 were in state 5. This optical pumping has been discussed previously (Wineland *et al.*, 1980; Hulet *et al.*, 1987) and studied experimentally (Hulet *et al.*, 1988). There are fluctuations about these average values, since any given ion is continually making transitions between states. The ions could have been completely optically pumped into state 4 by circularly polarized light propagating along the z axis, but this was not convenient experimentally.

The 313 nm beam was turned off to stop the optical pumping and to prevent perturbations to the $^9\mathrm{Be}^+$ energy levels. Next, the ions in state 4 were transferred to state 3 and then to state 2 by 0.2 s on-resonance rf pulses. These were π-pulses, that is, the products of the rf magnetic fields and the pulse durations were adjusted so that close to 100% of the ions were transferred in each step. The frequencies were approximately 320 712 280 Hz and 311 493 688 Hz for the $(4 \rightarrow 3)$ and $(3 \rightarrow 2)$ transitions, respectively. The Ramsey method of successive oscillatory fields was then used to create various superpositions of states 1 and 2 (Ramsey, 1956). The two Ramsey rf pulses were 0.5 s long and were separated by 5 s and the frequency was 303 016 377.265 Hz.

Then a measurement was made of the number of ions in state 2. First, the ions in state 2 were transferred to state 3 and then to state 4 by applying the π-pulses in the opposite order. Then the 313 nm beam was turned back on and the fluorescence photons were counted for 1 s.

The ions which were left in state 5 at the time that the 313 nm beam was turned off (about 1/17 of the total number) contribute to the fluorescence signal. This is so because the time constant for exchanging population between states 4 and 5 by spontaneous Raman transitions was around 0.1 s, which was less than the 1 s observation time.

Results

Ion plasmas containing numbers of $^9\mathrm{Be}^+$ ions ranging from a few to a few hundred were studied. Figures 5(a)–5(d) show the results from plasmas containing approximately 5, 21, 72, and 385 ions. The rf power for the $(2 \rightarrow 1)$ Ramsey resonance was adjusted so as to give a minimum fluorescence signal at the line center. Measurements were made at rf frequencies corresponding to the transition maximum (minimum fluorescence), the first upper and lower transition minima (maximum fluorescence), and the points halfway between the transition maximum and the upper and lower transition minima. The measured signal is the number of photons detected in the first second after the laser is turned on. This is

$$S = B + K(P_4 + P_5), \tag{4}$$

where B is the background signal, P_4 and P_5 are the numbers of ions in states 4 and 5, and K is a constant which must be calibrated for a given set of conditions. At the line center, the
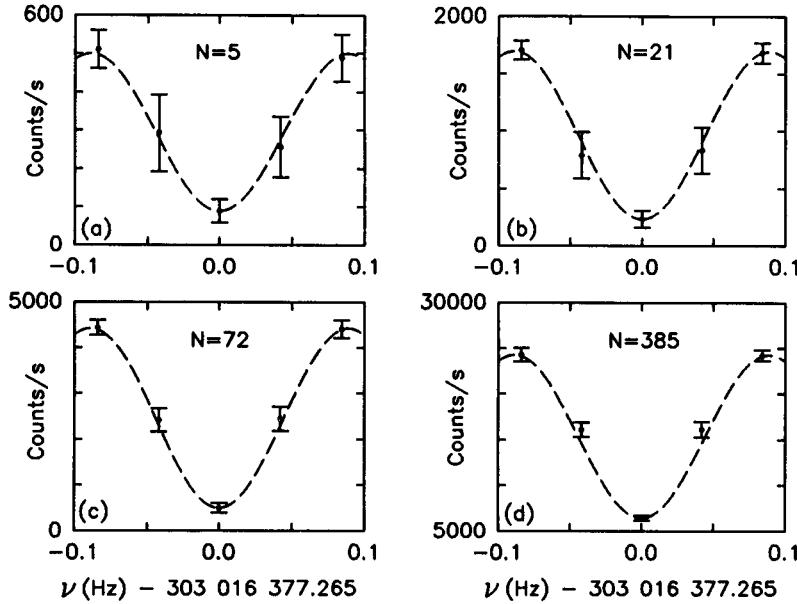
Figure 5: Plots of the fluorescence detected from ^{9}Be$^+$ ions confined in a Penning trap as a function of the frequency of the applied rf radiation for (a) 5 ions, (b) 21 ions, (c) 72 ions, and (d) 385 ions. The dots are the experimental mean signals, and the error bars show the experimental standard deviations. On the sides of the resonances, the standard deviations are mainly due to projection noise. The dashed lines show the calculated lineshapes, fitted to the experimental minimum and maxima.

signal is $B + KN/17$, where N is the total number of ^{9}Be$^+$ ions, while at the points of maximum fluorescence, it is $B + KN$. For the $N = 5$, 21, 72, and 385 data shown in Figs. 5(a)–5(d), $K = 87.3$, 73.9, 58.0, and 48.6 counts/ion, respectively. The fact that $K \gg 1$ for all of these cases means that projection noise should be more important than photon shot noise, except when the vanishing of one of the state amplitudes causes the projection noise to go to zero. In Figs. 5(a)–5(d), the dots are the experimental mean signals:

$$\overline{S} \equiv \frac{1}{n} \sum_{i=1}^{n} S_i, \tag{5}$$

where $S_1, S_2, \ldots, S_n$ is the sequence of measurements made under the same conditions. The error bars correspond to $\pm \sigma$, where σ was calculated from

$$\sigma^2 = \frac{1}{2(n-1)} \sum_{i=1}^{n-1} (S_{i+1} - S_i)^2. \tag{6}$$

Equation (6) was used, rather than the usual formula:

$$\sigma^2 = \frac{1}{n-1} \sum_{i=1}^{n} (S_i - \overline{S})^2, \tag{7}$$

because it is less sensitive to slow drifts of the signal, such as those caused by variations in the laser intensity or other experimental parameters.

Table 1: Mean signals and standard deviations for $N = 5, 21, 72,$ and 385 $^9Be^+$ ions. The terms "dip," "peaks," and "sides" refer to the points of minimum fluorescence, the points of maximum fluorescence, and the points halfway between the minimum and the maxima, respectively. The mean signal is $\overline{S}$, and the number of measurements is n. The measured standard deviation is σ_{exp}. The calculated standard deviation σ_{calc} is equal to $(\sigma_{proj}^2 + \sigma_{pump}^2 + \sigma_{shot}^2 + \sigma_{tech}^2)^{1/2}$. The value of σ_{exp} at the peaks was used to empirically determine σ_{tech}. Hence σ_{exp} must equal σ_{calc} at the peaks, but the agreement between σ_{exp} and σ_{calc} at the sides and at the dip is a test of the theory.

N	Position	n	$\overline{S}$ (counts)	σ_{exp}	σ_{proj}	σ_{pump}	σ_{shot}	σ_{tech}	σ_{calc}
5	dip	19	89	31	≈ 0	46	9	9	57
5	sides	38	275	81	95	23	17	26	105
5	peaks	38	500	53	≈ 0	≈ 0	22	48	53
21	dip	30	232	74	≈ 0	80	15	11	82
21	sides	60	810	194	164	40	28	37	175
21	peaks	60	1 693	87	≈ 0	≈ 0	41	77	87
72	dip	30	498	107	≈ 0	116	22	16	119
72	sides	60	2 432	247	239	58	49	79	263
72	peaks	60	4 429	159	≈ 0	≈ 0	67	144	159
385	dip	30	6 642	262	≈ 0	224	81	160	287
385	sides	60	16 108	774	463	112	127	388	627
385	peaks	60	24 253	605	≈ 0	≈ 0	158	584	605

Table 1 summarizes the data shown graphically in Figs. 5(a)–5(c). For each value of N, the data from the point of minimum fluorescence is labeled "dip," the data from the two points of maximum fluorescence are combined and labeled "peaks," and the data from the two points halfway between the minimum and the maxima are combined and labeled "sides."

Four contributions to σ are listed in Table 1: σ_{proj}, σ_{pump}, σ_{shot}, and σ_{tech}. They are assumed to be independent, so they are added in quadrature to yield σ_{calc}:

$$\sigma_{calc}^2 \equiv \sigma_{proj}^2 + \sigma_{pump}^2 + \sigma_{shot}^2 + \sigma_{tech}^2. \tag{8}$$

The projection noise σ_{proj} is assumed to be approximately zero at the peaks and at the dip and $(1/2)(16N/17)^{1/2}K$ on the sides. The factor of 16/17 appears in this expression because, on the average, 1/17 of the ions are left in state 5 by the optical pumping that precedes the rf pulses. The fluctuations in the number of ions left in state 5 are the source of σ_{pump}. This has the greatest effect at the dip, where the only contribution to the fluorescence is from the ions in state 5. At the dip,

$$\sigma_{pump} = [N(1/17)(16/17)]^{1/2} K = (4/17)\sqrt{N}K. \tag{9}$$

This is derived from the expression for the variance of a binomial distribution [see Eq. (2)]. At the peaks, σ_{pump} is approximately zero, because all of the ions are either in state 4 or state 5 and contribute to the signal. At the sides, σ_{pump} is half as large as at the dip. The shot noise σ_{shot} is equal to $(\overline{S})^{1/2}$ and results from Poisson statistics in the photon detection.

All other contributions to σ, such as those due to intensity fluctuations of the laser, are called technical noise σ_{tech}. Fluctuations in the shape and temperature of the ion plasma may make a
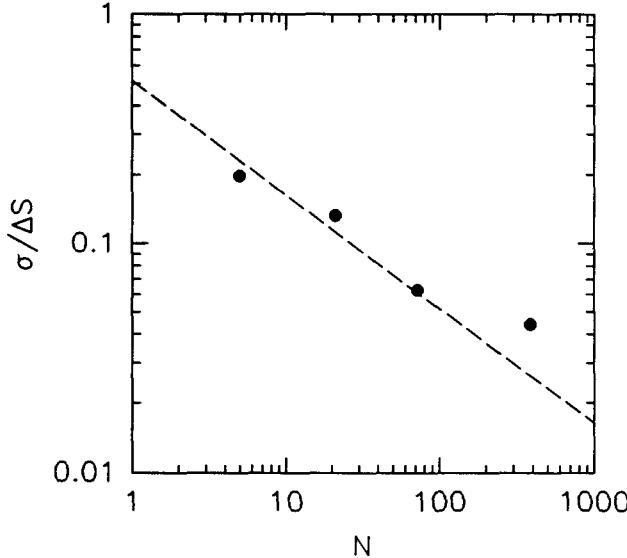
Figure 6: Plot of the normalized standard deviations as a function of N, the number of $^9\mathrm{Be}^+$ ions. The quantity $\sigma/\Delta S$ is the ratio of the experimental standard deviation on the sides of the resonance to the difference in the signal between the peaks and the dip. The dashed line is the theoretical prediction for the contribution from projection noise alone.

large contribution to σ_{tech}. Such fluctuations have been observed in other laser-cooled ion plasmas in Penning traps (Thompson et al., 1988; Itano et al., 1989), but are not well understood. Since σ_{tech} was not well understood theoretically, it was determined empirically from σ_{exp} at the peaks, where the only other contribution to σ is σ_{shot}, which is small. For $N = 5$, 21, 72, and 385, $\sigma_{\mathrm{tech}}/\overline{S}$ at the peaks was 9.6%, 4.5%, 3.2%, and 2.4%, respectively. The values of σ_{tech} at the sides and the dips were estimated by assuming that, for a given set of experimental conditions, σ_{tech} was proportional to $\overline{S}$.

The entries on Table 1 show that different types of noise dominate at each of the three positions on the line: σ_{proj} on the sides, σ_{pump} at the dip, and σ_{tech} at the peaks. Shot noise is not a large contribution for any of the cases shown in Table 1. Considering the uncertainties in the experimental parameters, particularly in N, the agreement between σ_{exp} and σ_{calc} is quite good. Figure 6 shows that the noise on the sides of the lines is mainly attributable to projection noise. The quantity plotted is $\sigma/\Delta S$ and is defined as

$$\frac{\sigma}{\Delta S} \equiv \frac{\sigma_{\mathrm{exp}}(\mathrm{sides})}{\overline{S}(\mathrm{peaks}) - \overline{S}(\mathrm{dip})}. \tag{10}$$

The dashed line is the theoretical prediction for projection noise alone:

$$\frac{\sigma_{\mathrm{proj}}}{\Delta S} = \frac{\sqrt{17}}{8\sqrt{N}} \approx \frac{0.515}{\sqrt{N}}. \tag{11}$$

The deviation of the experiment from theory for large N is due to technical noise. The ratio of the technical noise to the signal should be approximately constant as N increases, while the ratios of the other noise sources to the signal decrease as $1/\sqrt{N}$.

Discussion

The main features of projection noise in the $^9Be^+$ measurements are (1) it is greater at the sides than at the peaks and (2) its relative magnitude is proportional to $1/\sqrt{N}$. The data shows that the total noise at the sides is greater than the total noise at the peaks and that the total noise at the sides is proportional to $1/\sqrt{N}$. Feature (1) might also be caused by fluctuations in the frequency of the radiofrequency source or in the resonant frequency of the transition. However, this would not explain feature (2), since the relative magnitude would be independent of N. Also, previous measurements, made with much higher frequency resolution also rule out this possibility (Bollinger, 1991). The final piece of evidence that the noise at the sides is mainly due to projection noise is the quantitative agreement between the measured and calculated noise there.

The projection noise has been clearly observed on the sides of the resonances for values of N less than about 100. For larger values of N, projection noise is more difficult to observe and is easily obscured by other sources of noise in the present experiment.

ACKNOWLEDGMENTS

REFERENCES

Arecchi, F. T., Courtens, E., Gilmore, R., and Thomas, H. (1972) *Phys. Rev. A* **6**, 2211.

Bevington, P. R. (1969) *Data Reduction and Error Analysis for the Physical Sciences*, McGraw-Hill, New York.

Blatt, R., Gill, P., and Thompson, R. C. (1992) *J. Mod. Opt.* **39**, 193.

Bollinger, J. J., Heinzen, D. J., Itano, W. M., Gilbert, S. L., and Wineland, D. J. (1989) *Phys. Rev. Lett.* **63**, 1031.

Bollinger, J. J., Heinzen, D. J., Itano, W. M., Gilbert, S. L., Wineland, D. J. (1991) *IEEE Trans. Instrum. Meas.* **40**, 126.

Cutler, L. S., Giffard, R. P., and McGuire, M. D. (1981) In *Proc. 13th Annual Precise Time and Time Interval Applications and Planning Meeting*, NASA Conf. Publ. 2220, pp. 563–578.

Dehmelt, H. G. (1982) *IEEE Trans. Instrum. Meas.* **31**, 83.

Eriksen, P. and Poulsen, O. (1980) *J. Quant. Spectrosc. Radiat. Transfer* **23**, 599.

Gilbert, S. L., Bollinger, J. J., and Wineland, D. J. (1988) *Phys. Rev. Lett.* **60**, 2022.

Guern, Y., Bideau-Méhu, A., Abjean, R., and Johannin-Gilles, A. (1977) *Phys. Scripta* **14**, 273.

Hemmati, H., Bergquist, J. C., and Itano, W. M. (1983) *Opt. Lett.* **8**, 73.

Hulet, R. G. and Wineland, D. J. (1987) *Phys. Rev. A* **36**, 2758.

Hulet, R. G., Wineland, D. J., Bergquist, J. C., and Itano, W. M. (1988) *Phys. Rev. A* **37**, 4544.

Itano, W. M. and Wineland, D. J. (1982) *Phys. Rev. A* **25**, 35.

Itano, W. M., Bergquist, J. C., Hulet, R. G., and Wineland, D. J. (1987) *Phys. Rev. Lett.* **59**, 2732.

Itano, W. M., Brewer, L. R., Larson, D. J., Bollinger, J. J., Gilbert, S. L., and Wineland, D. J. (1989) in *Frequency Standards and Metrology*, Ed. De Marchi, A., p. 447, Springer-Verlag, Berlin.

Itano, W. M., Heinzen, D. J., Bollinger, J. J., and Wineland, D. J. (1990) *Phys. Rev. A* **41**, 2295.

Itano, W. M., Bergquist, J. C., Bollinger, J. J., Gilligan, J. M., Heinzen, D. J., Moore, F. L., Raizen, M. G., and Wineland, D. J. (1992) (in preparation).

Kitagawa, M. and Ueda, M. (1991) *Phys. Rev. Lett.* **67**, 1852; in *Noise in Physical Systems and 1/f Fluctuations*, Ed. Musha, T., Sato, S., and Yamamoto, M., p. 355, Ohmsha, Japan.

Larson, D. J., Bergquist, J. C., Bollinger, J. J., Itano, W. M., and Wineland, D. J. (1986) *Phys. Rev. Lett.* **57**, 70.

Ramsey, N. F. (1956) *Molecular Beams*, Oxford Univ. Press, London.

Raizen, M. G., Gilligan, J. M., Bergquist, J. C., Itano, W. M., and Wineland, D. J. (1992) *Phys. Rev. A* **45**, 6493.

Thompson, R. C., Barwood, G. P., and Gill, P. (1988) *Appl. Phys. B* **46**, 87.

Wineland, D. J., Bergquist, J. C., Itano, W. M., and Drullinger, R. E. (1980) *Opt. Lett.* **5**, 245.

Wineland, D. J., Bollinger, J. J., Itano, W. M., and Prestage, J. D. (1985) *J. Opt. Soc. Am. B* **2**, 1721.

Wineland, D. J. and Itano, W. M. (1987) *Phys. Today* **40** (6), 34.

Wineland, D. J., Bollinger, J. J., Itano, W. M., Moore, F. L., and Heinzen, D. J. (1992) (submitted for publication).

Yurke, B. (1986) *Phys. Rev. Lett.* **56**, 1515.

Yurke, B., McCall, S. L., and Klauder, J. R. (1986) *Phys. Rev. A* **33**, 4033.

Question (H. Rauch)

Are your ions in an uncertainty minimum state concerning momentum and localization within the trap?

Answer : Not in general. We cannot directly measure the position and momentum distributions precisely enough to verify that an ion is is a minimum uncertainty state However, in one experiment [F. Diedrich et al., Phys. Rev. Lett. 62, 403 (1989)] we have inferred by spectroscopic means that the ion was in the n=0 state of the quantum harmonic oscillator. The n=0 state is a minimum uncertainty state.